

Solvent Dependent Disproportionation of Cu(II) Complexes of N₂O₂-Type Ligands: Direct Evidence of Formation of Phenoxyl Radical: An Experimental and Computational Study

RAJIB KUMAR DEBNATH¹, APURBA KALITA², SOURAB SINHA³,
PRADIP KR. BHATTACHARYYA³, BIPLAB MONDAL² and JATINDRA NATH GANGULI^{1,*}

¹Department of Chemistry, Gauhati University, Guwahati-781 014, India

²Department of Chemistry, Indian Institute of Technology Guwahati, Guwahati-781 039, India

³Department of Chemistry, Arya Vidyapeeth College, Guwahati-781 016, India

*Corresponding author: E-mail: jatin_ganguli_gu@yahoo.co.in

Received: 24 March 2015;

Accepted: 20 May 2015;

Published online: 29 August 2015;

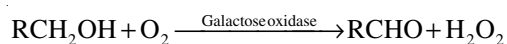
AJC-17496

Four Cu(II) complexes (**1**, **2**, **3** and **4**) with N₂O₂-type ligand, H₂L₁, H₂L₂, H₂L₃ and H₂L₄, respectively have been synthesized as the functional model for galactose oxidase. In presence of acetonitrile the Cu(II) centres in the complexes, undergo reduction with simultaneous oxidation of the ligands. The ligand oxidized products are isolated and characterized. Spectroscopic studies indicate that this disproportionation goes through the formation of a Cu(II)-phenoxyl intermediate. The complexes also undergoes the same reaction with pyridine, which indicates the involvement of the exergonic N-donor ligand for the formation of Cu(II)-phenoxyl complex. The Cu(II)-phenoxyl complexes are found to be stable in methanol in presence of a strong base. The paramagnetic centers in the Cu(II)-phenoxyl complexes were found to be weakly ferromagnetically coupled. The complexes, in acetonitrile solvent, have been found to oxidize primary alcohols to corresponding aldehydes. In absence of single crystal structures of the complexes, we optimized the structures using density functional theory (DFT). The UV-visible peaks of complexes as found from time dependent density functional theory (TDDFT) calculations match well with the observed experimental results.

Keywords: Galactose oxidase, N₂O₂ type ligands, Phenoxyl radical, DFT study.

INTRODUCTION

Galactose oxidase (GO), an extracellular copper-containing enzyme, is known to catalyze the two-electron oxidation of primary alcohols to the corresponding aldehydes with a simultaneous reduction of dioxygen to hydrogen peroxide¹⁻⁶.

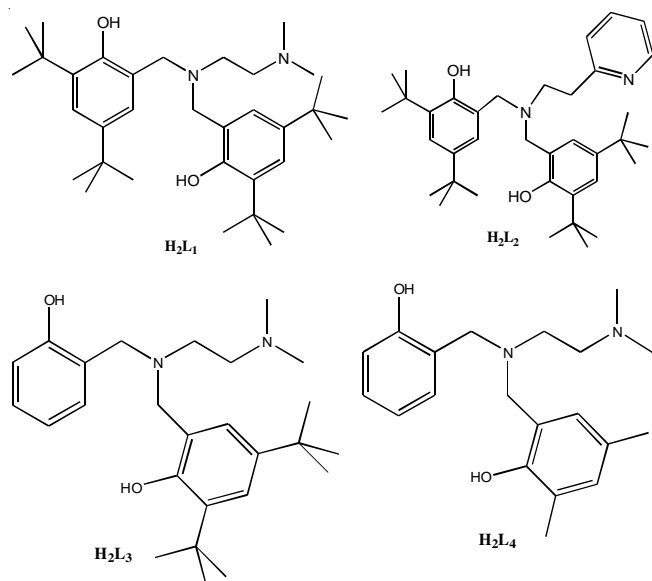


In contrast to other copper proteins which catalyze the multi-electron redox reactions, in galactose oxidase, an isolated monocopper center effects the two-electron redox process⁷⁻¹⁰. This paradox has been explained by the involvement of an additional redox center, a coordinated tyrosyl radical from the protein chain¹¹⁻¹⁴. Structural studies revealed that there are two distinct tyrosine residues in the active site of the inactive form of galactose oxidase; one of them is a cysteine modified phenol of tyrosine 272 which is coordinated to the copper center from equatorial position whereas the other phenol group is from tyrosine 495 that binds the metal from an apical position⁹. The proposed mechanistic cycle of the oxidation process involves Cu(I)-phenol and Cu(II)-phenoxyl radical states; however,

Cu(II)-phenolate form has not been detected in the catalytic process^{9,15,16}.

A number of model studies for the active site of galactose oxidase have been reported in last few years^{10,17-28}. Here we report our observation of the solvent dependent formation of mononuclear Cu(II)-phenoxyl radical complexes of *ortho*- and *para-tert*-butylated or methylated N₂O₂ ligands (Fig. 1) which appeared to be valuable functional models for galactose oxidase. At the same time, we observed that the reduction of the Cu(II) to Cu(I) in Cu(II)-phenoxyl complexes are accompanied by simultaneous decomposition of the ligands²⁹.

Density functional theory (DFT) has persistently substantiated its significance in solving problems based on molecular structure, providing platform to the researchers to explain the subject under investigation which are a bit challenging using experimental techniques³⁰. Time dependent density functional theory (TDDFT)³¹ is one of the fascinating tools provided by DFT to calculate the properties of molecules in its excited states. As we are unable to get good quality crystals for structure determination, we have used DFT and TDDFT to get information of structure and excited state chemistry of the complexes.

Fig. 1. Structure of N₂O₂ type ligands

COMPUTATIONAL METHODS

The geometrical minima of the species were optimized with 6-31G(d,p) basis set with Becke three parameter exchange and Lee, Yang and Parr correlation functional, B3LYP in gas phase. Real frequencies of the systems confirmed that they are at minima. Time dependent density functional theory calculations were performed using polarizable continuum model (PCM)⁸. All calculations were performed using Gaussian 09³².

EXPERIMENTAL

All reagents and solvents were purchased from commercial sources and were of reagent grade. Acetonitrile was distilled from calcium hydride. Deoxygenation of the solvent and solutions were affected by repeated vacuum/purge cycles or bubbling with nitrogen for 0.5 h. UV-visible spectra were recorded on a Perkin Elmer Lambda-25 spectrophotometer. FT-IR spectra were taken on a Perkin Elmer spectrophotometer with samples prepared as KBr pellets. Solution electrical conductivity was checked using a Systronic 305 conductivity bridge. ¹H NMR spectra were obtained with a 400 MHz Varian FT spectrometer. Chemical shifts (ppm) were referenced either with an internal standard (Me₄Si) for organic compounds or to the residual solvent peaks for copper complexes. The X-band electron paramagnetic resonance (EPR) spectrum of complex **1** and of the reaction mixture was recorded on a JES-FA200 ESR spectrometer, at room temperature as well as variable temperature. Elemental analyses were obtained from a Perkin Elmer Series II Analyzer. The magnetic moment of complex **1** is measured on a Cambridge Magnetic Balance.

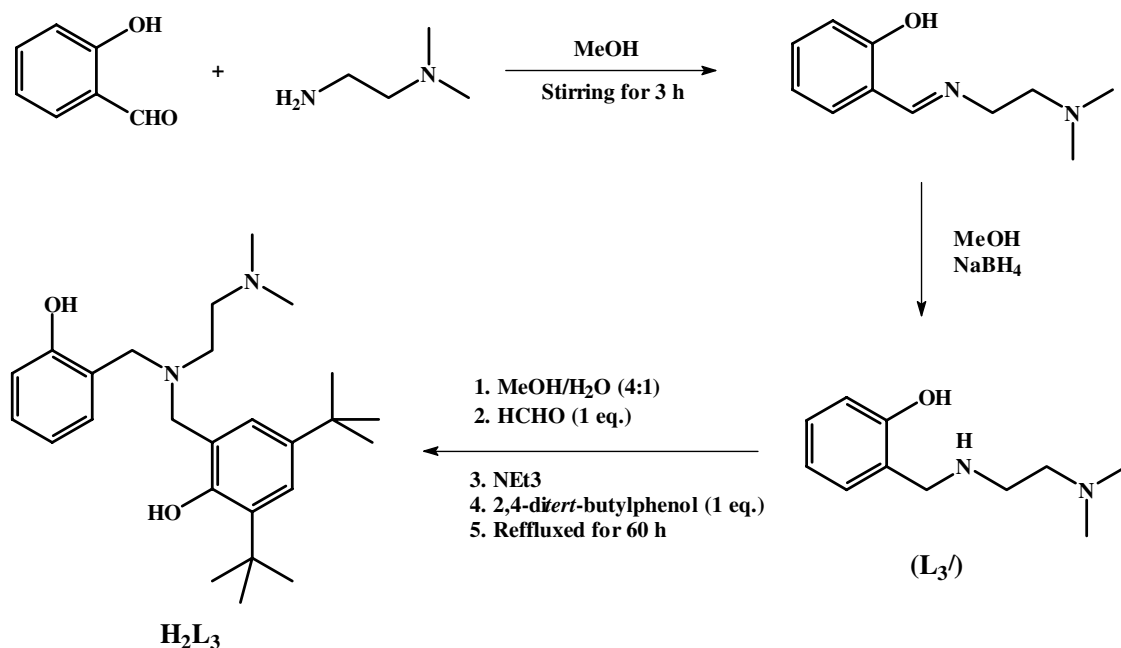
Crystal structure analysis: Single crystals were grown by slow diffusion followed by slow evaporation technique. The intensity data were collected using a Bruker SMART APEX-II CCD diffractometer, equipped with a fine focus 1.75 kW sealed tube MoK_α radiation ($\lambda = 0.71073 \text{ \AA}$) at 273(3) K, with increasing ω (width of 0.3° per frame) at a scan speed of 3 s/frame. The SMART software was used for data acquisition. Data integration and reduction were undertaken with SAINT

and XPREP software³³. Multi-scan empirical absorption corrections were applied to the data using the program SADABS³⁴. Structures were solved by direct methods using SHELXS-97 and refined with full-matrix least squares on F² using SHELXL-97³⁵. All non-hydrogen atoms were refined anisotropically. The hydrogen atoms were located from the difference Fourier maps and refined. Structural illustrations have been drawn with ORTEP-3 for Windows.

Synthesis of ligand H₂L₁ (Fig. 1) (C₃₄H₅₆N₂O₂): To a solution of 2,4-di-*tert*-butylphenol (4.80 g, 0.023 mol) in EtOH (15 mL) and water (3 mL) was added aqueous formaldehyde (37 %, 2.6 g, 0.032 mol), N,N-dimethyl-ethylenediamine (0.88 g, 0.010 mol) and triethylamine (0.500 mL, 0.004 mol) as a catalyst. The resulting solution was kept in an oil bath (at 50 °C) for 48 h. The white precipitate formed was filtered, washed with cold MeOH and dried under *vacuo* over P₂O₅. Yield: 4.586 g (75 %). Elemental analyses: Calcd. for C₃₄H₅₆N₂O₂: C, 77.21; H, 10.11; N, 5.87; O, 6.66. Found (%): C, 77.81; H, 10.76; N, 5.34; O, 6.10. ¹H NMR (400 MHz, CDCl₃), δ ppm 1.25(18H, s), 1.40(18H, s), 2.35(6H, s), 2.63(4H, t), 3.61(4H, s), 6.87(2H, s), 7.20(2H, s); ¹³C NMR (100 MHz, CDCl₃), δ ppm, 29.75, 31.91, 34.27, 35.22, 45.05, 49.25, 56.12, 56.77, 121.837, 123.53, 125.01, 136.28, 140.37, 153.47.

Synthesis of ligand H₂L₂ (Fig. 1) (C₃₇H₅₄N₂O₂): To a solution of 2,4-di-*tert*-butylphenol (4.80 g, 0.023 mol) in EtOH (15 mL) and water (3 mL) was added aqueous formaldehyde (37 %, 2.6 g, 0.032 mol), 2-(2-aminoethyl)pyridine (1.22 g, 0.010 mol) and triethylamine (0.500 mL, 0.004 mol) as a catalyst. The resulting solution was kept in an oil bath (at 50 °C) for 48 h. The white precipitate formed was filtered, washed with cold MeOH and dried under *vacuo* over P₂O₅. Yield: 4.680 g (72 %). Elemental analyses: Calcd. for C₃₇H₅₄N₂O₂: C, 79.56; H, 9.67; N, 5.02; O, 5.73. Found (%): C, 79.52; H, 9.74; N, 5.01; O, 5.73. ¹H NMR (400 MHz, CDCl₃), δ ppm, 1.25 (18H, s), 1.27 (18H, s), 2.75 (2H, t), 3.04 (2H, t), 3.66 (4H, s), 6.8 (2H, s), 6.97 (1H, d), 7.06 (2H, s), 7.17 (1H, t), 7.46 (1H, t), 8.60 (1H, d). ¹³C NMR (100 MHz, CDCl₃), δ ppm, 29.83, 31.90, 34.08, 35.13, 54.17, 57.11, 121.80, 122.09, 123.43, 123.72, 125.5, 136.31, 137.66, 140.60, 149.07, 153.19, 159.18.

Synthesis of ligand H₂L₃ (Fig. 1) (C₂₆H₄₀N₂O₂): (Schiff base reaction) One equivalent of N,N-dimethylethane-1,2-diamine (1.76 g, 20 mmol) and equivalent amount of salicylaldehyde (2.44 g, 20 mmol) in methanol was stirred for 3 h. A yellow coloured imine was formed. The imine was reduced with 2.5 equivalents of sodium borohydride (1.90 g, 50 mmol). After complete reduction a colourless solution was obtained. The solution was stirred for 1 h. Then it was neutralized by acetic acid to pH 7 and was extracted with chloroform to afford L₃' (yield: 2.30 g, about 60 %). The L₃' (0.97 g, 5 mmol) was dissolved in methanol-water mixture (1:4), one equivalent of formaldehyde (0.15 g, 5 mmol), one equivalent of triethylamine (0.50 g, 5 mmol) and one equivalent of 2,4-di-*tert*-butylphenol (1.03 g, 5 mmol) was added into reaction mixture and refluxed for 3 days at 60 °C. A white precipitate was observed, it was filtered, washed with water and dried (yield: 1 g, about 50 %) (**Scheme-I**). The NMR signals of H₂L₃ are as follows: ¹H NMR (400 MHz, CDCl₃), δ ppm 1.25 (18H, s), 1.40 (18H, s), 2.35 (6H, s), 2.63 (4H, t), 3.61 (4H, s), 6.87



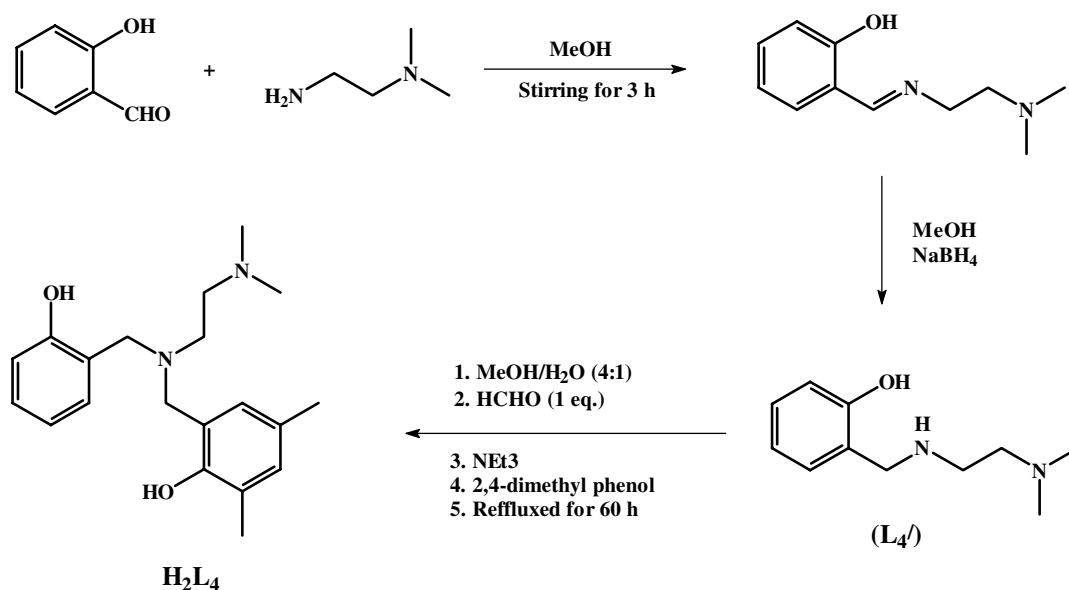
Scheme-I

(2H, s), 7.20 (2H, s); ¹H NMR (100 MHz, CDCl₃), δ ppm, 29.75, 31.91, 34.27, 35.22, 45.05, 49.25, 56.12, 56.77, 121.837, 123.53, 125.01, 136.28, 140.37, 153.47.

Synthesis of ligand H₂L₄ (Fig. 1) (C₂₀H₂₈N₂O₂): The Schiff base reaction was carried out using one equivalent of N,N-dimethyl-ethane-1,2-diamine (1.76 g, 20 mmol) and equivalent amount of salicylaldehyde (2.44 g, 20 mmol) in methanol medium. A yellow coloured imine was formed. The imine was reduced with 2.5 equivalents of sodium borohydride (1.90 g, 50 mmol). After complete reduction a colourless solution was obtained. The solution was stirred for 1 h. Then it was neutralized by acetic acid to pH 7 and was extracted with chloroform to afford L₄' (yield: 2.30 g, about 60 %). The L₄' (0.97 g, 5 mmol) was dissolved in methanol-water mixture (1:4), one equivalent of formaldehyde (0.15 g, 5 mmol), one equivalent of

triethylamine (0.50 g, 5 mmol) and one equivalent of 2,4-dimethylphenol (0.61 g, 5 mmol) was added into reaction mixture and refluxed for 3 days at 60 °C. A white precipitate appears, it was filtered, washed with water and dried (yield: 0.82 g, about 50 %) (**Scheme-II**). The NMR signals of H₂L₄ are as follows: ¹H NMR (400 MHz, CDCl₃), δ ppm, 1.25 (18H, s), 1.27 (18H, s), 2.75 (2H, t), 3.04 (2H, t), 3.66 (4H, s), 6.8 (2H, s), 6.97 (1H, d), 7.06 (2H, s), 7.17 (1H, t), 7.46 (1H, t), 8.60 (1H, d). ¹³C NMR (100 MHz, CDCl₃), δ ppm, 29.83, 31.90, 34.08, 35.13, 54.17, 57.11, 121.80, 122.09, 123.43, 123.72, 125.5, 136.31, 137.66, 140.60, 149.07, 153.19, 159.18.

Synthesis of complex 1 [CuL₄(CH₃OH)]: 0.370 g (1.0 mmol) of [Cu^{II}(H₂O)₆](ClO₄)₂ was dissolved in 10 mL distilled methanol. To this solution, 0.524 g (1 mmol) of the ligand H₂L₄ was added slowly with constant stirring. The colour of



Scheme-II

the solution turned into violet from light blue. The stirring was continued for 1 h at 298 K. The volume of the solution then reduced to about 2 mL and kept it overnight at 273 K. This resulted into violet colour microcrystalline precipitate of complex **1**. Yield: 0.588 g (63.36 %). Elemental analyses: Calcd. for CuC₃₄H₅₆N₂O₂: C, 69.39; H, 9.52; N, 4.76. Found (%): C, 69.41; H, 9.59; N, 4.76. ESI-mass (*m/z*) = 588.30, magnetic susceptibility = χ_M , 1.20 B.M.

Synthesis of complex 2 [CuL₂(CH₃OH)]: 0.370 g (1.0 mmol) of [Cu^{II}(H₂O)₆](ClO₄)₂ was dissolved in 10 mL distilled methanol solvent. To this solution, 0.558 g (1.0 mmol) of the ligand H₂L₂ was added slowly with constant stirring. The colour of the solution turned into violet from light blue. The stirring was continued for 1 h at 298 K. The volume of the solution then reduced to about 2 mL and kept it overnight at 273 K. The violet colour complex **2** was obtained as microcrystalline precipitate. Yield: 0.622 g (67 %). Elemental analyses: Calcd. for CuC₃₇H₅₄N₂O₂: C, 71.38; H, 8.68; N, 4.50. Found (%): C, 70.40; H, 8.75; N, 4.50. ESI-mass (*m/z*) = 621.35 and molar susceptibility = χ_M , 1.28 B.M.

Synthesis of complex 3 [CuL₃(CH₃OH)]: 0.370 g (1 mmol) of [Cu^{II}(H₂O)₆](ClO₄)₂ was dissolved in 10 mL distilled MeOH. To this solution, 0.412 g (1 mmol) of the ligand H₂L₃ was added slowly with constant stirring. The colour of the solution turned into green from light blue. The stirring was continued for 1 h at 298 K. The volume of the solution then reduced to about 2 mL. To this, 10 mL of benzene was added to make a layer on it and kept it overnight at 273 K. This resulted into green colour crystal of complex **3**. Yield: 0.594 g (80.45 %). Elemental analyses: Calcd. for C₂₇H₄₁CuN₂O₃: C, 64.19; H, 8.18; N, 5.55; Found (%): C, 64.56; H, 8.12; N, 5.43. Molar conductivity: [$\Lambda_M = 23 \text{ W}^{-1} \text{ cm}^2 \text{ mol}^{-1}$]. ESI-mass (*m/z*) = 505.61, magnetic susceptibility = χ_M , 1.28 B.M.

Synthesis of complex 4 [CuL₄(CH₃OH)]: 0.370 g (1 mmol) of [Cu^{II}(H₂O)₆](ClO₄)₂ was dissolved in 10 mL distilled MeOH. To this solution, 0.328 g (1 mmol) of the ligand H₂L₄ was added slowly with constant stirring. The colour of the solution turned into green from light blue. The stirring was continued for 1 h at 298 K. The volume of the solution then reduced to about 2 mL. To this, 10 mL of benzene was added to make a layer on it and kept it overnight on freezer. This resulted into green colour crystal of complex **4**. Yield: 0.512 g (82.23 %). Elemental analyses: Calcd. for C₂₁H₂₉CuN₂O₃: C, 59.91; H, 6.94; Cu, 15.09; N, 6.65; O, 11.40; Found (%): C, 59.77; H, 7.05; N, 6.73; O, 11.64; Cu, 14.81. Molar conductivity: [$\Lambda_M = 37 \text{ W}^{-1} \text{ cm}^2 \text{ mol}^{-1}$]. ESI-mass (*m/z*) = 421.14, magnetic susceptibility = χ_M , 1.33 B.M.

Isolation of L₁': 185 mg (0.5 mmol) of [Cu(H₂O)₆](ClO₄)₂ was dissolved in 15 mL acetonitrile in a round bottom flask. 262 mg (0.5 mmol) of the ligand H₂L₁ was added to it and stirred for 1 h. The transient greenish solution became orange in course of reaction. The volume of the solution was reduced using rotavapour and was kept at 273 K for overnight. [Cu(CH₃CN)₄](ClO₄) was crystallized out. The remaining part was then dried and subjected to column chromatography. The 3,5-di-*tert*-butyl-2-hydroxybenzaldehyde was separated by hexane, yield (75 %). The amine product, L₁', was eluted with methanol:chloroform (v/v, 1:10) mixture. Yield (70 %). 3,5-di-*tert*-butyl-2-hydroxybenzaldehyde: ¹H NMR (400 MHz,

CDCl₃), δ ppm, 1.33(9H, s), 1.43 (9H, s), 7.35 (1H, s), 7.60 (1H, s), 9.86 (1H, s), 11.66 (1H, s); ¹³C NMR (100 MHz, CDCl₃), δ ppm, 29.46, 31.52, 34.50, 35.21, 120.18, 128.05, 132.09, 95 137.67, 141.81, 159.29, 197.55. For L₁', ¹H NMR (400 MHz, CDCl₃), δ ppm; 1.28 (9H, s), 1.40 (9H, s), 2.39 (6H, s), 2.69(4H, t), 3.66 (2H, s), 6.90 (1H, s), 7.20(1H, s); ¹³C NMR (100 MHz, CDCl₃), δ ppm, 29.88, 31.80, 34.45, 35.06, 45.87, 49.37, 51.56, 82.09, 119.18, 122.09, 136.78, 142.22, 150.83.

Isolation of L₂': 185 mg (0.5 mmol) of [Cu(H₂O)₆](ClO₄)₂ was dissolved in 15 mL acetonitrile in a round bottom flask. 280 mg (0.5 mmol) of the ligand H₂L₂ was added to it and stirred for 1 h. The transient green solution became yellow and finally converted into the course of reaction. The volume of the solution is then reduced using rotavapour and was kept at 273 K for overnight. [Cu(CH₃CN)₄](ClO₄) was crystallized out. The solution was then dried and subjected to column chromatographic separation. The 3,5-di-*tert*-butyl-2-hydroxybenzaldehyde was eluted first by hexane and the amine product, L₂', was eluted with 10 % methanol in chloroform mixture. For L₂', ¹H NMR (400 MHz, CDCl₃), δ ppm, 1.25 (9H, s), 1.27 (9H, s), 1.15, 2.70 (2H, t), 3.08 (2H, t), 3.68 (2H, s), 6.8 (2H, s), 6.97 (1H, d), 7.09 (1H, s), 7.15 (1H, t), 7.49 (1H, t), 8.62 (1H, d). ¹³C NMR (100 MHz, CDCl₃), δ ppm, 29.75, 31.75, 34.11, 34.96, 54.03, 56.92, 121.68, 121.94, 123.25, 123.60, 125.30, 136.13, 137.63, 140.41, 148.86, 153.02, 159.05.

Isolation of L₃'/L₄': 185 mg (0.5 mmol) of [Cu(H₂O)₆](ClO₄)₂ was dissolved in 15 mL acetonitrile in a round bottom flask. 206 mg (0.5 mmol) of the ligand H₂L₃ or 164 mg (0.5 mmol) of the ligand H₂L₄ was added to it and stirred for 1 h. The transient green solution became yellow and finally converted into the course of reaction. The volume of the solution is then reduced using rotavapour and was kept at 273 K for overnight. [Cu(CH₃CN)₄](ClO₄) was crystallized out. The solution was then dried and subjected to column chromatographic separation. The 3,5-di-*tert*-butyl-2-hydroxybenzaldehyde (for H₂L₃) and 3,5-di-methyl-2-hydroxybenzaldehyde (for H₂L₄) was eluted first by hexane and the amine product, L₃' or L₄' was eluted with 10 % methanol in chloroform mixture. For L₃' or L₄' ¹H NMR (400 MHz, CDCl₃), δ ppm, 2.05 (6H, s), 2.22 (2H, t), 2.31 (2H, t), 2.95 (1H, s), 3.90 (2H, s), 7.02 (1H, t), 7.13 (1H, t), 7.29 (1H, d), 8.22 (1H, d), ¹³C NMR (100 MHz, CDCl₃), δ ppm, 44.25, 45.38, 54.51, 59.96, 77.03, 122.04, 126.08, 136.13, 149.25, 160.01.

RESULTS AND DISCUSSION

The ligands, H₂L₁, H₂L₂, H₂L₃ and H₂L₄ have been synthesized using previously reported method of one-pot Mannich synthesis³⁶⁻³⁸. The formation of both the ligands have been confirmed by various spectroscopic techniques like FT-IR, ¹H NMR and ¹³C NMR, elemental analysis and single crystal structures. The X-ray quality single crystals of the ligands, H₂L₁, H₂L₂, H₂L₃ and H₂L₄ were grown by the slow diffusion of dichloromethane solutions of the ligand into hexane followed by slow evaporation at 298 K. The ORTEP diagrams of the neutral H₂L₁, H₂L₂, H₂L₃ and H₂L₄ molecules are shown in Fig. 2. The crystallographic data, bond angle and bond length for neutral H₂L₁, H₂L₂, H₂L₃ and H₂L₄ molecules are shown in Tables 1-3, respectively.

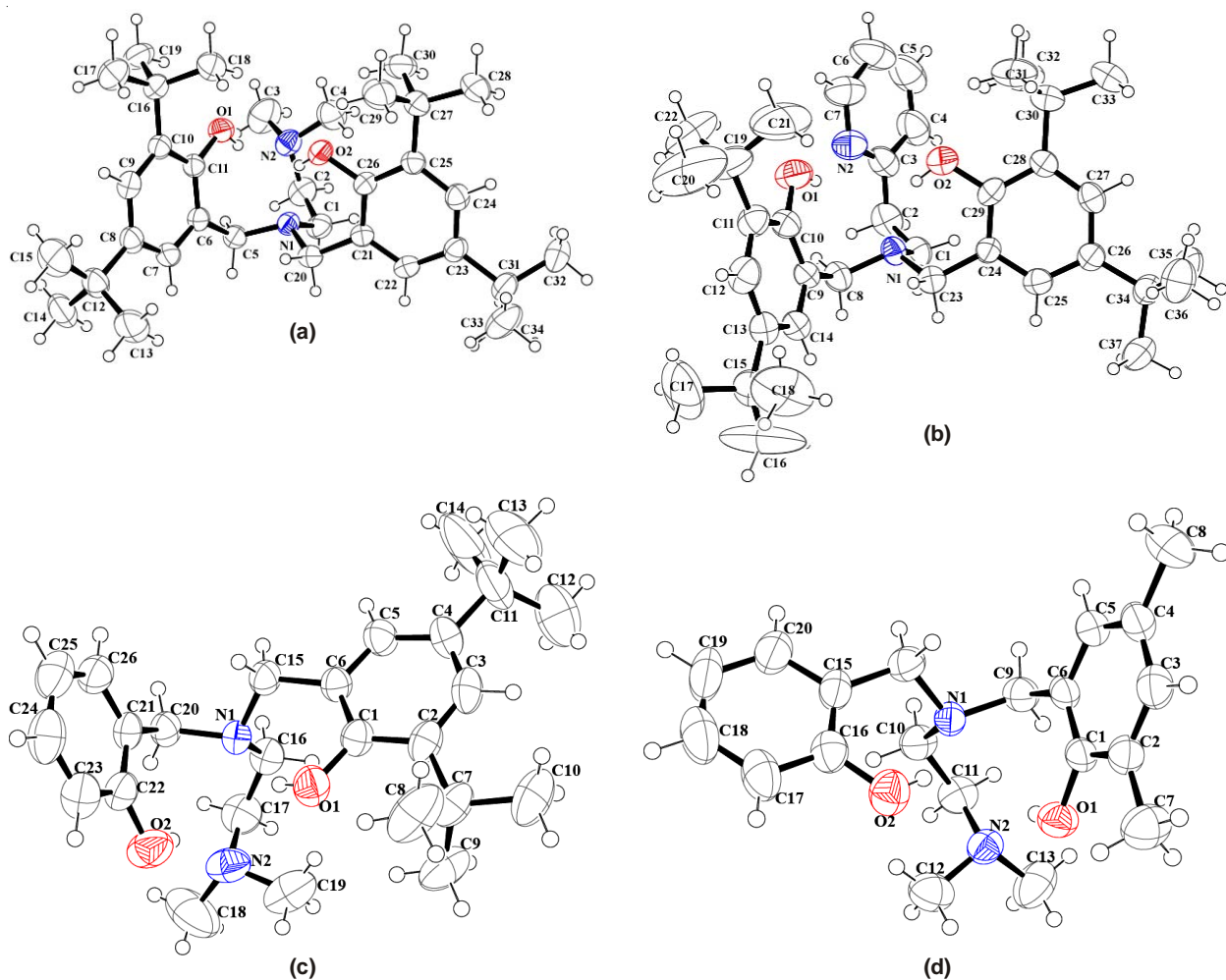


Fig. 2. ORTEP diagram of the ligands: (a) H_2L_1 (b) H_2L_2 (c) H_2L_3 and (d) H_2L_4 (50 % thermal ellipsoid)

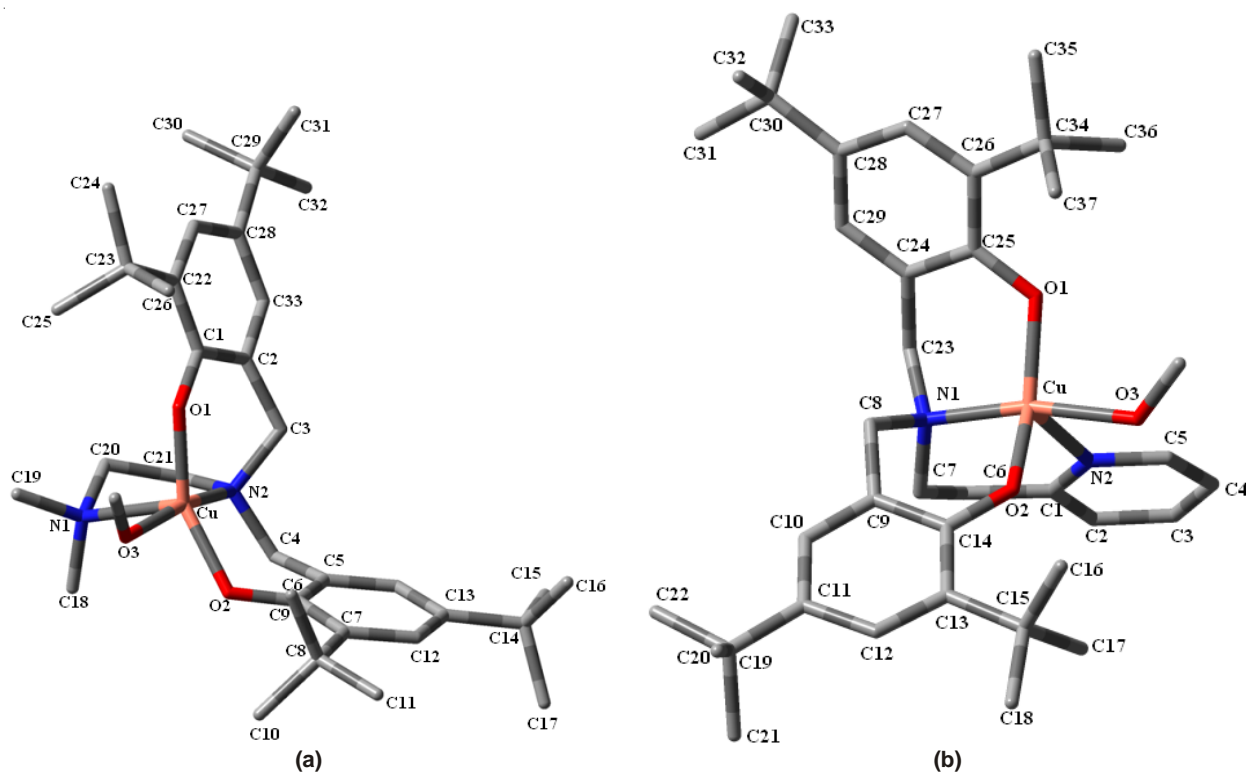


Fig. 3. Optimized structure of (a) complex 1 and (b) complex 2 at 6-31G (d,p) level of theory (for better visualization, H-atoms from the structure has been omitted)

TABLE-1
 CRYSTALLOGRAPHIC DATA OF LIGANDS H₂L₁, H₂L₂, H₂L₃ AND H₂L₄

Parameters	H ₂ L ₁	H ₂ L ₂	H ₂ L ₃	H ₂ L ₄
Formulae	C ₃₄ H ₅₆ N ₂ O ₂	C ₃₇ H ₅₄ N ₂ O ₂	C ₂₆ H ₄₀ N ₂ O ₂	C ₂₀ H ₂₈ N ₂ O ₂
m.w. (g)	524.81	558.82	412.59	328.44
Crystal system	Monoclinic	Tetragonal	Monoclinic	Monoclinic
Space group	P2(1)/c	I4(1)/a	P21/c	P21/c
Temperature (K)	296(2)	296(2)	296(2)	296(2)
Wavelength (Å)	0.71073	0.71073	0.71073	0.71073
a (Å)	15.3374(9)	27.9655(10)	12.314(4)	9.9314(5)
b (Å)	100.036(4)	27.9655(10)	13.416(4)	13.9518(7)
c (Å)	21.7414(13)	17.7352(7)	15.629(4)	14.4574(7)
α (°)	90.00	90.00	90.00	90.004(3)
β (°)	100.047(2)	90.00	96.895(6)	108.314(3)
γ (°)	90.00	90.00	90.00	90.016(3)
V (Å ³)	3399.2(4)	13870.2(9)	2563.3(13)	1901.76(16)
Z	4	16	4	4
Density (Mg m ⁻³)	1.025	1.070	1.069	1.147
Abs. coefficient (mm ⁻¹)	0.062	0.065	0.067	0.128
F(000)	1160.0	4896.0	904.0	712
Total no. of reflections	23171	41097	17936	24158
Reflections, I > 2σ(I)	3554	2403	4586	3376
Max. 2θ (°)	28.36	25.00	28.40	28.30
Ranges (h, k, l)	-20 ≤ h ≤ 20 -11 ≤ k ≤ 13 -28 ≤ l ≤ 28	-28 ≤ h ≤ 22 -30 ≤ k ≤ 32 -19 ≤ l ≤ 21	-16 ≤ h ≤ 15 -17 ≤ k ≤ 17 -20 ≤ l ≤ 20	-12 ≤ h ≤ 12 -16 ≤ k ≤ 16 -19 ≤ l ≤ 17
Complete to 2θ (%)	97.00	93.50	98.10	81.60
Refinement method	Full-matrix least-squares on F ²			
Data/Restraints/Parameters	8249 / 0 / 360	5731/0/384	6321 / 0 / 281	4630/0/223
WR ₂ (all data)	0.1620	0.0795	0.1603	0.1312
Goof (F ²)	0.944	1.818	0.774	0.862
R indices [I > 2σ(I)]	0.0535	0.0650	0.0581	0.0485
R indices (all data)	0.1473	0.1841	0.1617	0.1221

 TABLE2
 SELECTED BOND LENGTH (Å) OF
 LIGANDS H₂L₁, H₂L₂, H₂L₃ AND H₂L₄

Bond length (Å)	H ₂ L ₁	H ₂ L ₂	H ₂ L ₃	H ₂ L ₄
N(1)-C(1)	1.464(2)	1.468(3)	1.464(2)	1.468(3)
N(1)-C(5)	1.472(2)	-	1.472(2)	-
N(1)-C(8)	-	1.482(2)	-	1.482(2)
N(1)-C(20)	1.469(2)	-	1.469(2)	-
N(1)-C(23)	-	1.468(3)	-	1.468(3)
N(2)-C(2)	1.458(3)	-	1.458(3)	-
N(2)-C(3)	1.459(3)	1.332(3)	1.459(3)	1.332(3)
N(2)-C(4)	1.459(3)	-	1.459(3)	-
N(2)-C(7)	-	1.336(4)	-	1.336(4)
O(1)-C(11)	1.369(2)	-	1.369(2)	-
O(1)-C(26)	1.370(2)	-	1.370(2)	-
O(1)-C(10)	-	1.372(3)	-	1.372(3)
O(2)-C(29)	-	1.374(3)	-	1.374(3)

Since we could not grow good quality crystals for single crystal X-ray analysis, optimized structures of the complexes were obtained using DFT at B3LYP/6-31G (d,p) level of theory using Gaussian 09³². The optimized structure of complexes **1** and **2** are shown in Fig. 3 and the shapes of HOMO are presented in Fig. 4. The calculated values of bond lengths and bond angles are shown in Tables 4 and 5, respectively. The density functional studies showed that the complexes adopt distorted square pyramidal geometry at the copper center. Some of the key parameters of the complexes such as the bond length

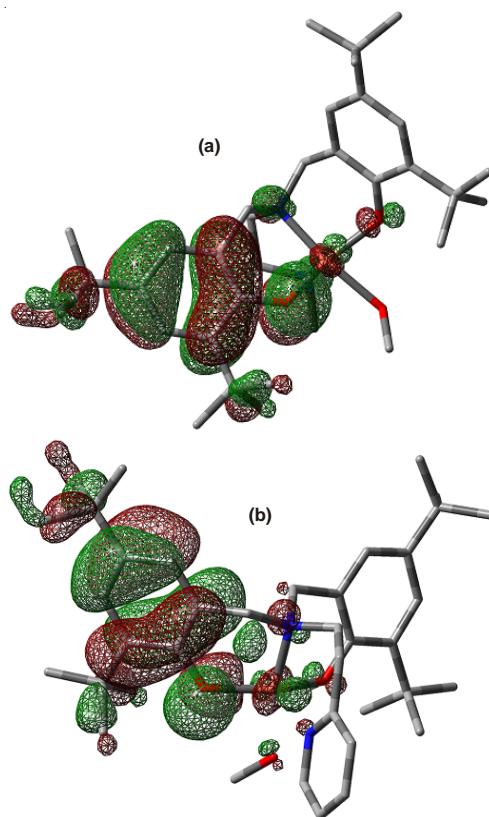

 Fig. 4. HOMO of (a) complex **1** and (b) complex **2**, respectively

TABLE-3
SELECTED BOND ANGLES (°) FOR LIGANDS H₂L₁, H₂L₂, H₂L₃ AND H₂L₄

Bond angle (°)	H ₂ L ₁	H ₂ L ₂	H ₂ L ₃	H ₂ L ₄
C(1)-N(1)-C(5)	112.41(15)	-	112.41(15)	-
C(1)-N(1)-C(8)	-	109.60(2)	-	109.60(2)
C(1)-N(1)-C(20)	110.97(14)	-	110.97(14)	-
C(20)-N(1)-C(5)	111.10(14)	-	111.10(14)	-
C(23)-N(1)-C(1)	-	109.70(2)	-	109.70(2)
C(23)-N(1)-C(8)	-	111.10(2)	-	111.10(2)
C(2)-N(2)-C(4)	111.18(18)	-	111.18(18)	-
C(2)-N(2)-C(3)	110.50(2)	-	110.50(2)	-
C(3)-N(2)-C(7)	-	117.20(3)	-	117.20(3)
C(4)-N(2)-C(3)	110.04(19)	-	110.04(19)	-
N(1)-C(1)-C(2)	113.61(16)	114.80(2)	113.61(16)	114.80(2)
N(1)-C(5)-C(6)	111.78(15)	-	111.78(15)	-
N(1)-C(20)-C(21)	112.33(15)	-	112.33(15)	-
N(1)-C(8)-C(9)	-	113.20(2)	-	113.20(2)
N(1)-C(23)-C(24)	-	113.20(2)	-	113.20(2)
N(2)-C(3)-C(2)	112.63(17)	-	112.63(17)	-
N(2)-C(3)-C(4)	-	117.40(4)	-	117.40(4)
N(2)-C(7)-C(6)	-	122.60(4)	-	122.60(4)
N(2)-C(2)-C(1)	-	124.30(4)	-	124.30(4)
O(1)-C(11)-C(6)	121.55(17)	-	121.55(17)	-
O(1)-C(11)-C(10)	117.79(17)	-	117.79(17)	-
O(1)-C(10)-C(9)	-	121.00(3)	-	121.00(3)
O(1)-C(10)-C(11)	-	117.70(3)	-	117.70(3)
O(2)-C(26)-C(21)	119.33(16)	-	119.33(16)	-
O(2)-C(26)-C(25)	119.29(16)	-	119.29(16)	-
O(2)-C(29)-C(24)	-	119.00(3)	-	119.00(3)
O(2)-C(29)-C(28)	-	119.10(3)	-	119.10(3)

TABLE-4
IMPORTANT BOND LENGTHS OF COMPLEXES 1, 2, 3 AND 4 (OBTAINED FROM DFT STUDY)

Complex 1	Bond length (Å)	Complex 2	Bond length (Å)	Complex 3	Bond length (Å)	Complex 4	Bond length (Å)
Cu1-N1	2.36	Cu1-N1	2.35	Cu1-N1	2.36	Cu1-N1	2.35
Cu1-N2	2.01	Cu1-N2	1.98	Cu1-N2	2.01	Cu1-N2	1.98
Cu1-O1	1.90	Cu1-O1	1.90	Cu1-O1	1.90	Cu1-O1	1.90
Cu1-O2	1.94	Cu1-O2	1.94	Cu1-O2	1.94	Cu1-O2	1.94
Cu1-O3	2.10	Cu1-O3	2.13	Cu1-O3	2.10	Cu1-O3	2.13
O1-C1	1.32	O1-C25	1.33	O1-C1	1.32	O1-C25	1.33
O2-C6	1.33	O2-C1	1.33	O2-C6	1.33	O2-C1	1.33
N1-C18	1.47	N1-C8	1.49	N1-C18	1.47	N1-C8	1.49
N2-C3	1.50	N2-C1	1.34	N2-C3	1.50	N2-C1	1.34
C2-C3	1.51	C1-C2	1.40	C2-C3	1.51	C1-C2	1.40

TABLE-5
IMPORTANT BOND ANGLES OF COMPLEXES 1, 2, 3 AND 4 (OBTAINED FROM DFT STUDY)

Complex 1	Bond angle (°)	Complex 2	Bond angle (°)	Complex 3	Bond angle (°)	Complex 4	Bond angle (°)
N1-Cu1-O1	102	N1-Cu1-O1	98	N1-Cu1-O1	95	N1-Cu1-O1	96
N2-Cu1-O1	97	N2-Cu1-O1	108	N2-Cu1-O1	97	N2-Cu1-O1	94
N1-Cu1-O2	114	N1-Cu1-O2	94	N1-Cu1-O2	116	N1-Cu1-O2	111
N2-Cu1-O2	96	N2-Cu1-O2	108	N2-Cu1-O2	97	N2-Cu1-O2	96
O1-Cu1-O2	142	O1-Cu1-O2	140	O1-Cu1-O2	146	O1-Cu1-O2	150
O2-Cu1-O3	77	O2-Cu1-O3	75	N1-Cu1-O3	92	N1-Cu1-O3	99
Cu1-O1-C1	127	Cu1-O1-C25	124	Cu1-O1-C1	126	Cu1-O1-C1	127
Cu1-O2-C6	119	Cu1-O2-C14	128	Cu1-O2-C6	118	Cu1-O2-C6	113
N2-C2-C3	115	O1-Cu1-O3	93	N2-C3-C2	114	N2-C3-C2	115
Cu1-N2-C3	105	Cu1-N1-C7	112	Cu1-N2-C3	105	Cu1-N2-C3	106

of Cu1-O1 (1.90), Cu1-O2 (1.94) for complex 1, Cu1-O1 (1.94), Cu1-O2 (1.90) for complex 2, Cu1-O1 (1.89), Cu1-O2 (1.92) for complex 3 and Cu1-O1 (1.89), Cu1-O2 (1.93) for complex 4 obtained after optimization are, are comparable to bond length data obtained from X-ray crystal structure of related galactose oxidase model complexes^{6,13}.

The conductivity study shows that the complexes are non-ionic in nature and the IR study shows that the ligand to metal binding is phenolate in nature. The ESI-mass study shows that the absence of perchlorate in the complexes.

UV-visible spectral studies: The complexes 1, 2, 3 and 4 in methanol solution, display absorptions in UV-visible region

characteristic to the typical square-pyramidal phenolato-Cu(II) charge transfer. Fig. 5 shows the representative spectrum of complex **2** in methanol solvent. The O_{phenolato} → Cu^{II} charge transfer bands appear at 490 ($\epsilon = 1430 \text{ M}^{-1} \text{ cm}^{-1}$) and 497 nm ($\epsilon = 1270 \text{ M}^{-1} \text{ cm}^{-1}$), 490 ($\epsilon = 987 \text{ M}^{-1} \text{ cm}^{-1}$) and 442 nm ($\epsilon = 1146 \text{ M}^{-1} \text{ cm}^{-1}$) in case of **1**, **2**, **3** and **4**, respectively^{39,40}.

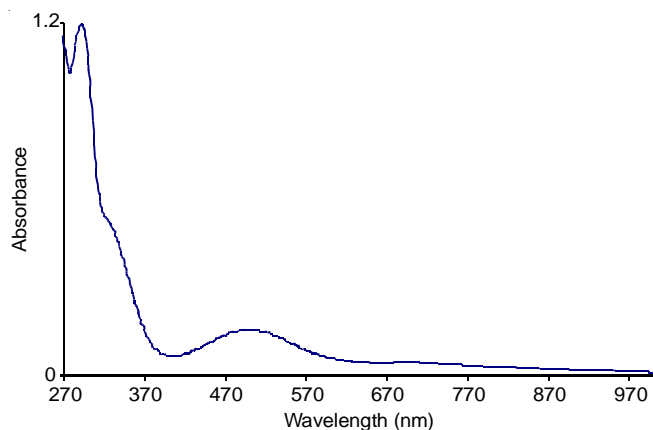


Fig. 5. UV-visible spectrum of complex **2** in methanol at room temperature

However, the phenolate Cu(II) transition, in dry and distilled acetonitrile has been found to decrease in intensity very rapidly which is attributed to the reduction of Cu(II) to Cu(I) (Fig. 6) presumably through the very unstable Cu(II)-phenoxy radical complex²⁹.

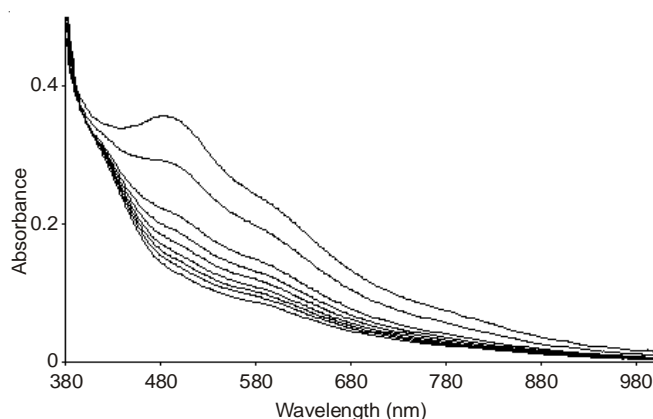


Fig. 6. UV-visible monitoring of the formation of Cu(II)-phenoxy radical complex by the addition of acetonitrile in methanolic solution of complex **1**

It has been found that these phenoxy radical species are thermally unstable. However, they are found to be stable in presence of base (NaOEt) (Fig. 7)²⁹.

It has been found that addition of pyridine instead of acetonitrile to the methanolic solution of complexes **1**, **2**, **3** and **4** at room temperature also results into the gradual decrease in intensity of the O_{phenolato} → Cu^{II} charge transfer bands. This fact can be attributed to the reduction of Cu(II) center to Cu(I) *via* the formation of intermediate Cu(II)-phenoxy radical complex (Fig. 8). However, we are not able to trap the Cu(II)-phenoxy radical complex in this case because of the rapid rate of reaction at room temperature. These results indicate that the exergonic nitrogen donor ligands/solvents play an important role to initiate the Cu(II)-phenoxy radical complex formation.

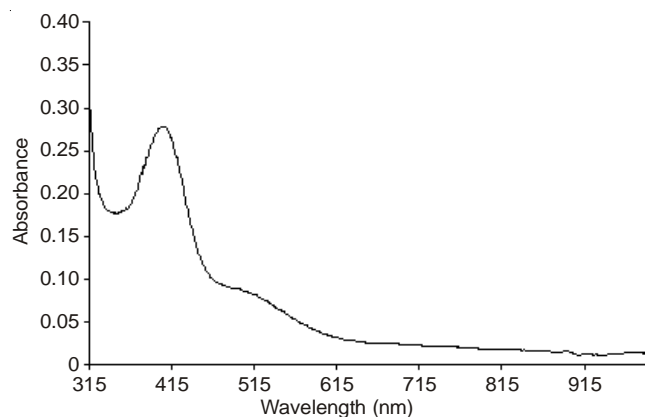


Fig. 7. UV-visible spectrum of Cu(II)-phenoxy radical complex generated from complex **1** in methanol in presence of NaOEt

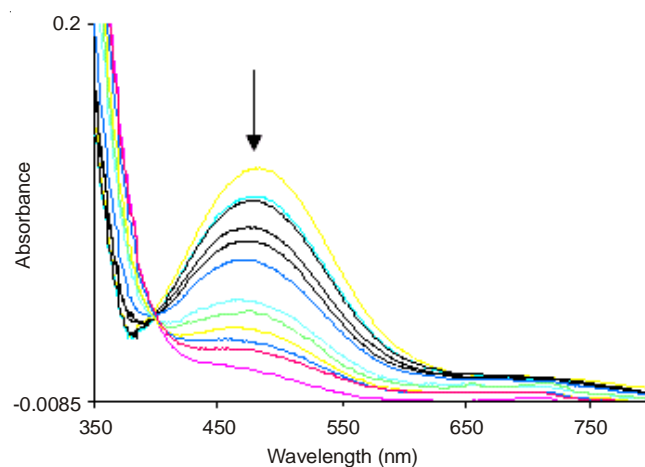


Fig. 8. UV-visible spectral monitoring of the reduction of Cu(II) in [L₂Cu^{II}] in presence of pyridine in methanol solvent. The intensity of the phenolate → Cu^{II} charge transfer band at about 500 nm decreases with time in presence of pyridine ([L₂Cu^{II}]:Pyridine = 1:5)

In order to assign the UV-visible spectra, we performed TDDFT calculations on the optimized structures of the complexes at B3LYP/6-31G(d,p) level of theory in methanol using the PCM model⁴¹. The calculated wavelength (λ_{cal}), major molecular orbitals involved in the transitions, oscillator strengths (f) and coefficients of the wave function corresponding to a particular transition (Φ_c) along with the experimental values of the wavelengths (λ_{exp}) are given in Table-6.

Time dependent density functional theory calculations confirmed that, in complex **1** there is one intense band at 481.22 nm with a high oscillator strength ($f = 0.0126$). This peak is close to the experimentally observed peak at 497 nm. There is also a weak band at 523.85 nm (with $f = 0.0094$), the 481.22 nm band originates mainly from the HOMO-2 → HOMO transition with a large coefficient (0.5544) for this complex. However for complexes **2** and **4**, we observed intense bands at 465 nm and 487 nm (with $f = 0.0032$ and 0.0416 respectively) which are in well accord with the experimentally observed peaks. There are also some weak bands arising at 536 and 418 nm (with $f = 0.0261$ and 0.0032). The 465 and 487 nm bands (in complexes **2** and **4**, respectively) originate mainly from the molecular orbitals HOMO-2 → HOMO and HOMO-1 → HOMO respectively and have the largest coefficients (0.6639 and 0.7534, respectively). Interestingly, in complex **3**, one

TABLE-6
CALCULATED WAVELENGTHS (nm), MAJOR ORBITALS INVOLVED, OSCILLATOR STRENGTH (f) AND COEFFICIENTS OF THE WAVE FUNCTION CORRESPONDING TO A PARTICULAR TRANSITION (Φ_c) OBTAINED FROM THE TD-DFT CALCULATIONS IN ADDITION WITH THE EXPERIMENTAL RESULTS

Complexes	λ_{cal} (nm)	Orbitals involved	f	Φ_c	λ_{exp} (nm)
1	481	HOMO-2 \rightarrow HOMO	0.0126	0.55444	497
2	465	HOMO-2 \rightarrow HOMO	0.0032	0.66393	490
	536*	HOMO-1 \rightarrow HOMO	0.0261	0.71122	
3	490	HOMO-1 \rightarrow HOMO	0.0417	0.75535	490
	420*	HOMO-2 \rightarrow HOMO	0.0032	0.65192	
4	487*	HOMO-1 \rightarrow HOMO	0.0416	0.75340	442
	418	HOMO-2 \rightarrow HOMO	0.0032	0.65299	

** No experimental peaks observed.

intense peak at 490 nm is in concurrence with the experimental data which arises from the transition from HOMO-1 \rightarrow LUMO, having oscillation strength ($f = 0.0032$) and coefficient (0.7553).

EPR studies: The X-band EPR spectra in methanol solution of **1**, **2**, **3** and **4** at 298 K exhibit axial four line spectra characteristic to $S = 1/2$ signals with Cu-hyperfine splitting²⁹. The spectral features are typical to the square-pyramidal Cu^{II} -complexes. The calculated parameters are as follows. Complex **1**, $g_{\parallel} = 2.285$; $g_{\perp} = 2.022$; $A = 109 \times 10^{-4} \text{ cm}^{-1}$; complex **2**, $g_{\parallel} = 2.310$; $g_{\perp} = 2.065$; $A = 110 \times 10^{-4} \text{ cm}^{-1}$, Complex **3**, $g_{\parallel} = 2.297$; $g_{\perp} = 2.031$; $A = 111 \times 10^{-4} \text{ cm}^{-1}$; complex **4**, $g_{\parallel} = 2.335$; $g_{\perp} = 2.073$; $A = 113 \times 10^{-4} \text{ cm}^{-1}$. These values match well with those reported for similar model compounds of the inactive form of galactose oxidase^{10,18,19,21,42-44}.

It is interesting to note that in acetonitrile solvent, the complexes display two distinct signals in X-band EPR at room temperature which is characteristic of spin triplet state with very weak ferromagnetic coupling^{7,11,29}. One signal appears at $g = 2.06$ as a broad one for Cu(II) center and other one is very sharp isotropic signal for organic radical at $g = 1.99$ characteristic of phenoxyl radical (Fig. 5).

The broad signal for Cu(II) and the radical signal have been found to be disappeared with time and with equal proportion indicating an immediate reaction between the Cu(II) center and phenoxyl radical (Fig. 9). This further supports the formation of only one phenoxyl radical though there are two phenolate groups. Shimazaki *et al.* have reported that N_2O_2 type tripod ligands with stoichiometric amounts of Cu(II) perchlorate results into a Cu(II) phenoxyl radical and Cu(I) in disproportionation reaction^{29,45-48}. On the other hand, Stack *et al.*⁴⁹ have reported Cu(III) complexes by disproportionation of Cu(II). Our present observations clearly indicate that the disproportionation take place through Cu(II) phenoxyl radical complex formation. Shimazaki *et al.*⁴⁶ have also suggested that a dimeric intermediate plays a key role in the copper(II) disproportionation.

On the other hand, in absence of base, the green solution which has been observed after addition of acetonitrile to the methanolic solution of **1**, **2**, **3** and **4** readily turned colourless in air at room temperature and yielded the colourless crystals of $[\text{Cu}(\text{CH}_3\text{CN})_4]\text{ClO}_4$. This reaction has been found to take place even under dinitrogen condition; which indicates that the radical formation is not due to the oxidation by oxygen. These reductions are found to be associated with the concomitant

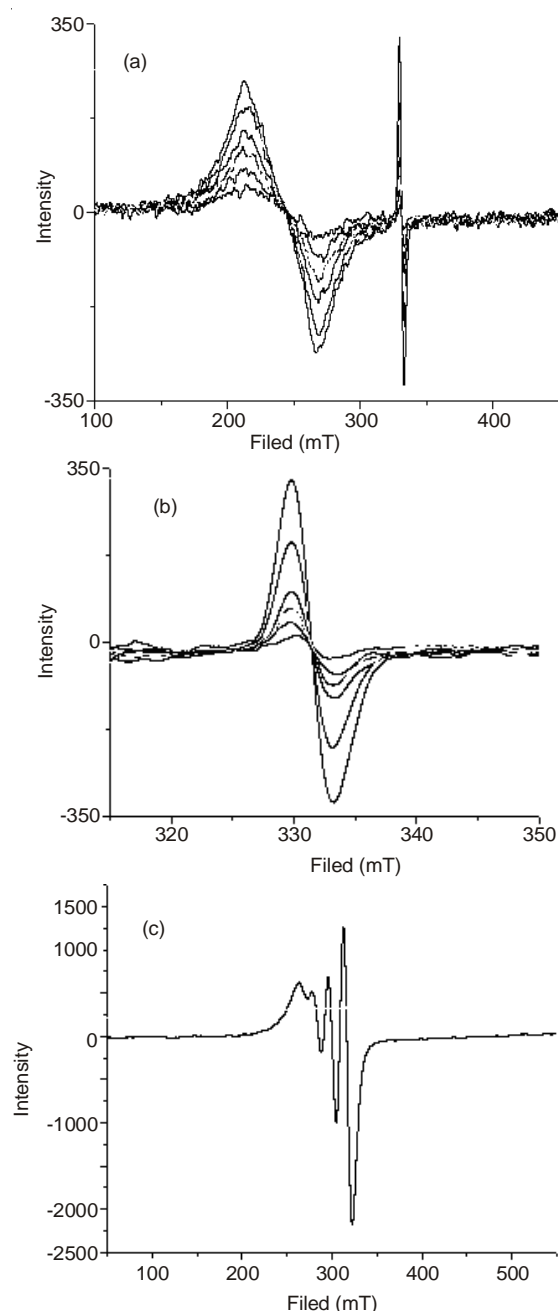


Fig. 9. (a) X-band EPR spectrum of the Cu(II)-phenoxyl radical complex generated from complex **1** in acetonitrile at room temperature. The signals were found to decrease in intensity rapidly with time. (b) The sharp radical signal of (a). (c) X-band EPR spectrum of complex **1** in methanol

decomposition of the ligands H₂L₁, H₂L₂, H₂L₃ and H₂L₄ to L₁['], L₂['], L₃['] and L₄['], respectively along with 3,5-di-*tert*-butyl-2-hydroxybenzaldehyde in case of H₂L₁, H₂L₂, H₂L₃ and 3,5-dimethyl-2-hydroxybenzaldehyde in case of H₂L₄ (Scheme-III)²⁹.

Galactose oxidase reactivity: The radical complexes generated from complexes **1**, **2**, **3** and **4** are observed to oxidize primary alcohols to corresponding aldehydes successfully. A number of substituted benzyl alcohols have been found to result into corresponding aldehydes when stirred with complex **1** in acetonitrile solvent (Table-7)³⁸. The same reaction has not been observed in methanol solvent even after stirring for 24 h in presence of air at room temperature. However, addition of few drops of acetonitrile to the methanolic solution leads to the oxidation. This can be attributed to the fact that in presence of acetonitrile the Cu(II)-phenoxy radical forms, which actively takes part in the oxidation of the primary alcohols. The complexes **2**, **3** and **4** have also been observed to induce the same reaction with a variable turn over numbers.

Conclusion

The present study demonstrates a new set of Cu(II) complexes with N₂O₂-type ligand as the functional model for galactose oxidase active site. It has been found that the Cu(II) centers in the complexes, in presence of acetonitrile, undergo reduction with a concomitant oxidation of the ligands. The ligand oxidized products are isolated and characterized. Spectroscopic studies indicate that this disproportionation goes through the formation of a Cu(II)-phenoxy intermediate. Instead of acetonitrile, pyridine can also results into the same reaction which indicates the involvement of the exergonic N-donor ligand for the formation of Cu(II)-phenoxy complex. The Cu(II)-phenoxy complex is found to be stable in methanol in presence of base. The complexes show galactose oxidase activity to oxidize primary alcohols to corresponding aldehydes in acetonitrile solvent. The present study demonstrates examples of the formation of Cu(II)-phenoxy complex where the paramagnetic centers are very weakly coupled. A distorted square pyramidal geometry of the complexes is confirmed by DFT

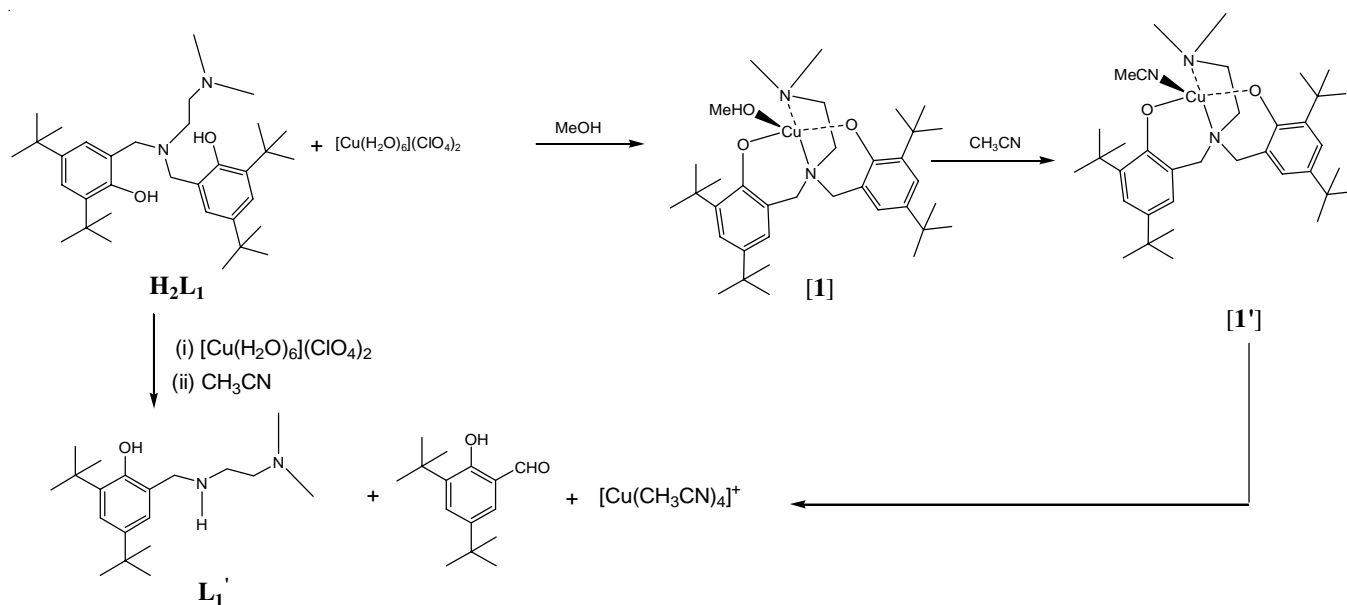


TABLE-7
SELECTED PRIMARY ALCOHOLS AND THEIR OXIDATION PRODUCTS
AFTER REACTION WITH COMPLEXES 1-4 IN ACETONITRILE

S. No.	Reactant alcohol	Product aldehyde*	TON for 1	TON for 2	TON for 3	TON for 4
1			210	210	175	165
2			230	230	185	170
3			170	170	155	145

*All the products have been quantified by GC.

study. The HOMO of the complexes associated one of the phenol rings. The TDDFT calculations of the complexes are well matched with the experimental value.

ACKNOWLEDGEMENTS

The authors acknowledge to CSIR for financial support to R.K. Debnath. Thanks are also due to DST-FIST for single crystal X-ray, CIF, IIT Guwahati for NMR & Mass spectrophotometer, Arya Vidyapeeth College for conducting DFT study and Department of Chemistry for providing the necessary research facilities.

REFERENCES

- D. Amaral, F. Kelly-Falcoz and B.L. Horecker, *Methods Enzymol.*, **9**, 87 (1966).
- P.S. Tressel and D.J. Kosman, *Methods Enzymol.*, **89**, 163 (1982).
- R.A. vander Meer, J.A. Jongejan and J.A. Duine, *J. Biol. Chem.*, **264**, 7792 (1989).
- J.W. Whittaker, in eds.: M.H. Sigel and A. Sigel, *Metalloenzymes Involving Amino Acid Residue and Related Radicals*, Marcel Dekker, New York, vol. 30, 315 (1994).
- P.F. Knowles and N. Ito, *Perspective Bio-inorg. Chem.*, **2**, 207 (1994).
- J.W. Whittaker, in eds.: K.D. Karlin and Z. Tyeklar, *Bioinorganic Chemistry of Copper*, Chapman & Hall, Inc. New York, p. 447 (1993).
- N. Ito, S.E.V. Phillips, C. Stevens, Z.B. Ogel, M.J. McPherson, J.N. Keen, K.D.S. Yadav and P.F. Knowles, *Nature*, **350**, 87 (1991).
- N. Ito, S.E.V. Phillips, C. Stevens, Z.B. Ogel, M.J. McPherson, J.N. Keen, K.D.S. Yadav and P.F. Knowles, *Faraday Discuss.*, **93**, 75 (1992).
- N. Ito, S.E.V. Phillips, K.D.S. Yadav and P.F. Knowles, *J. Mol. Biol.*, **238**, 704 (1994).
- J.A. Halfen, B.A. Jazdzewski, S. Mahapatra, L.M. Berreau, E.C. Wilkinson, L. Que Jr. and W.B. Tolman, *J. Am. Chem. Soc.*, **119**, 8217 (1997).
- D.J. Kosman, M.J. Ettinger, R.E. Weiner and E.J. Massaro, *Arch. Biochem. Biophys.*, **165**, 456 (1974).
- M.M. Whittaker and J.W. Whittaker, *J. Biol. Chem.*, **263**, 6074 (1988).
- M.M. Whittaker and J.W. Whittaker, *J. Biol. Chem.*, **265**, 9610 (1990).
- J.W. Whittaker, *Chem. Rev.*, **103**, 2347 (2003).
- J.W. Whittaker, *Met. Ions Biol. Syst.*, **30**, 315 (1994).
- J. Stubbe and W.A. Van der Donk, *Chem. Rev.*, **98**, 705 (1998).
- M. Taki, H. Kumei, S. Nagatomo, T. Kitagawa, S. Itoh and S. Fukuzumi, *Inorg. Chim. Acta*, **300**, 622 (2000).
- A. Sokolowski, H. Leutbecher, T. Weyhermuller, R. Schnepf, E. Bothe, E. Bill, P. Hildebrandt and K. Wieghardt, *J. Biol. Inorg. Chem.*, **2**, 444 (1997).
- C. Ochs, F.E. Hahn and R. Frohlich, *Eur. J. Inorg. Chem.*, 2427 (2001).
- Y. Wang, J.L. DuBois, B. Hedman, K.O. Hodgson and T.D.P. Stack, *Science*, **279**, 537 (1998).
- Y. Wang and T.D.P. Stack, *J. Am. Chem. Soc.*, **118**, 13097 (1996).
- P. Chaudhuri, M. Hess, J. Müller, K. Hildenbrand, E. Bill, T. Weyhermüller and K. Wieghardt, *J. Am. Chem. Soc.*, **121**, 9599 (1999).
- P. Chaudhuri, M. Hess, T. Weyhermuller and K. Wieghardt, *Angew. Chem.*, **111**, 1165 (1999).
- D. Zurita, I. Gautier-Luneau, S. Ménage, J.-L. Pierre and E. Saint-Aman, *J. Biol. Inorg. Chem.*, **2**, 46 (1997).
- S. Itoh, M. Taki, S. Takayama, S. Nagatomo, T. Kitagawa, N. Sakurada, R. Arakawa and S. Fukuzumi, *Angew. Chem.*, **111**, 2944 (1999).
- M. Vaidyanathan, M. Palaniandavar and R.S. Gopalan, *Inorg. Chim. Acta*, **324**, 241 (2001).
- M. Vaidyanathan, R. Viswanathan, M. Palaniandavar, T. Balasubramanian, P. Prabhakaran and P.T. Muthiah, *Inorg. Chem.*, **37**, 6418 (1998).
- B.A. Jazdzewski and W.B. Tolman, *Coord. Chem. Rev.*, **200-202**, 633 (2000).
- R.K. Debnath, P. Kumar, A. Kalita, B. Mondal and J.N. Ganguli, *Polyhedron*, **51**, 222 (2013).
- W. Koch and M.C. Holthausen, *A Chemist's Guide to Density Functional Theory*, edn 2, Wiley-VCH, New York (2001).
- G. Scalmani, M.J. Frisch, B. Mennucci, J. Tomasi, R. Cammi and V. Barone, *J. Chem. Phys.*, **124**, 94107 (2006).
- Gaussian 09, Revision B.01, Gaussian, Inc., Wallingford CT (2010).
- SMART, SAINT and XPREP, Siemens Analytical X-ray Instruments Inc., Madison, Wisconsin, USA (1995).
- G.M. Sheldrick, SADABS: Software for Empirical Absorption Correction, University of Göttingen, Institut für Anorganische Chemieder Universität, Tammanstrasse 4, D-3400 Göttingen, Germany (1999–2003).
- G.M. Sheldrick, SHELXS-97, University of Göttingen, Germany (1997).
- G. Dutta, R.K. Debnath, A. Kalita, P. Kumar, M. Sarma, R.B. Shankar and B. Mondal, *Polyhedron*, **30**, 293 (2011).
- E.Y. Tshuva, I. Goldberg, M. Kol and Z. Goldschmidt, *Inorg. Chem.*, **40**, 4263 (2001).
- H. Sopo, A. Lehtonen and R. Sillanpää, *Polyhedron*, **27**, 95 (2008).
- J.A. Halfen, V.G. Young and W.B. Tolman, *Angew. Chem.*, **108**, 1832 (1996).
- E. Bill, J. Muller, T. Weyhermuller and K. Wieghardt, *Inorg. Chem.*, **38**, 5795 (1999).
- J. Tomasi, B. Mennucci and R. Cammi, *Chem. Rev.*, **105**, 2999 (2005).
- D. Zurita, C. Scheer, J.-L. Pierre and E. Saint-Aman, *Dalton Trans.*, 4331 (1996).
- S. Itoh, S. Takayama, R. Arakawa, A. Furuta, A.M. Komatsu, A. Ishida, S. Takamuku, S. Fukuzumi, Electronic Effect of the Thioether Group in the Novel Organic Cofactor, *Inorg. Chem.*, **36**, 1407 (1997).
- M.A. Halcrow, L.M.L. Chia, J.E. Davies, X. Liu, L.J. Yellowlees, E.J. L. McInnes and F.E. Mabbs, *Chem. Commun.*, 2465 (1998).
- F. Michel, F. Thomas, S. Hamman, E. Saint-Aman, C. Bucher and J.-L. Pierre, *Chem. Eur. J.*, **10**, 4115 (2004).
- Y. Shimazaki, S. Huth, A. Odani and O. Yamauchi, *Angew. Chem.*, **39**, 1666 (2000).
- F. Michel, S. Torelli, F. Thomas, C. Duboc, C. Philouze, C. Belle, S. Hamman, E. Saint-Aman and J.-L. Pierre, *Angew. Chem.*, **44**, 438 (2005).
- Y. Shimazaki, S. Huth, S. Hirota and O. Yamauchi, *Inorg. Chim. Acta*, **331**, 168 (2002).
- X. Ribas, D.A. Jackson, B. Donnadieu, J. Mahia, T. Parella, R. Xifra, B. Hedman, K.O. Hodgson, A. Llobet and T.D.P. Stack, *Angew. Chem.*, **114**, 3117 (2002).